

ARTICLE

Mineral Composition and Distribution of Silt and Oxides in Shatt Al-Arab Deposits, Basra, Iraq

Salah Mahdi AL- Hameedawi* , Raid Shaalan Jarallah

Department of Soil Science and Water Resources, College of Agriculture, University of Al-Qadisiyah, Al-Qadisiyah 58002, Iraq

ABSTRACT

Understanding the mineral composition and distribution of river deposits is crucial for environmental management, resource utilization, and geological studies. This study aims to investigate the mineral composition and distribution of silt and oxides in the deposits of the Shatt al-Arab River, specifically in the Faw area of Basra Governorate. Samples were collected from depths of 0–30, 30–60, and 60–90 cm. The silt fraction (2–53 micrometers) was isolated, and mineral analysis was conducted using XRD and a point-counting device. Morphological characteristics were determined using a polarized light microscope. XRD analysis revealed the presence of minerals such as quartz, calcite, dolomite, smectite, kaolinite, chlorite, illite, hematite, magnetite, and albite at varying depths. Polarized light microscopy identified additional minerals within light and heavy fractions. The study found a dominance of monocrystalline quartz and opaque minerals, with magnetite being more prevalent than hematite across all depths and a high correlation coefficient with depth (0.96). Depth-specific variations in mineral composition suggest the need for further research in different locations and at greater depths. These findings provide insights into sedimentary processes and potential resource utilization in the region, making this study significant for regional geological and environmental research. Future research should focus on the temporal changes in mineral composition and their impact on sediment dynamics to enhance the understanding of regional geological history and resource management.

Keywords: Sand; Mineral composition; Shatt al-Arab; Tigris; Euphrates

*CORRESPONDING AUTHOR:

Salah Mahdi AL- Hameedawi, Department of Soil Science and Water Resources, College of Agriculture, University of Al-Qadisiyah, Al-Qadisiyah 58002, Iraq; Email: agr22.mas4@qu.edu.iq

ARTICLE INFO

Received: 12 July 2024 | Revised: 22 July 2024 | Accepted: 22 July 2024 | Published: 12 September 2024
DOI: <https://doi.org/10.30564/jees.v6i3.6870>

CITATION

Mahdi AL- Hameedawi, S., Jarallah, R.S., 2024. Mineral Composition and Distribution of Silt and Oxides in Shatt Al-Arab Deposits, Basra, Iraq. *Journal of Environmental & Earth Sciences*. 6(3): 83-91. DOI: <https://doi.org/10.30564/jees.v6i3.6870>

COPYRIGHT

Copyright © 2024 by the author(s). Published by Bilingual Publishing Co. This is an open access article under the Creative Commons Attribution-NonCommercial 4.0 International (CC BY-NC 4.0) License (<https://creativecommons.org/licenses/by-nc/4.0/>).

1. Introduction

These Weathering indices are extensively utilized in soil science and related environmental disciplines for diverse applications, including soil classification, studies on soil formation dynamics, and broader research on past climatic conditions. These indices are broadly classified into two main categories: geochemical and mineralogical^[1]. Geochemical weathering is the process in which the chemical composition of the parent material is altered by weathering conditions, leading to the loss of soluble and mobile elements and the relative concentration of less soluble and immobile elements in the soil^[2]. This process is crucial for palaeoclimate reconstructions, soil formation studies, soil classification, and assessing human impacts on soil composition. On the other hand, mineralogical weathering refers to the process by which the mineral composition of a soil or rock changes over time due to exposure to atmospheric and environmental conditions^[3]. This process involves the breakdown and alteration of minerals, leading to the formation of new minerals and affecting the soil's physical and chemical properties. Mineralogical weathering indices are used to study these changes, providing insights into soil formation, classification, and environmental conditions.

The geochemical method falls short in accounting for the movement of authigenic components throughout the soil profile, leading to variations in geochemistry and consequently different W values. Another drawback of the geochemical approach is its inability to accurately differentiate between changes caused by natural weathering processes and those induced by human activities, potentially leading to misinterpretations in soil studies and palaeoclimate reconstructions^[4,5]. While the mineralogical approach to soil evaluation cannot fully replace the geochemical approach, it can provide quick and broad insights into soil characteristics^[6]. Mineralogical analysis directly identifies and quantifies the minerals present in soil, offering valuable information about soil genesis, weathering processes, and environmental conditions^[7]. This approach helps in understanding the physical and structural changes in soil, which are crucial for studying soil formation and classification.

The mineral composition of soils in a specific region is significantly impacted by the geological formations beneath it. The inherent physical and chemical properties of diverse

soils are shaped by the clay mineral composition and the environmental conditions present during their formation^[8]. In some cases, widespread of minerals in the soil makes it difficult to predict the provenance determination. For example,^[9] identified difficulties in anticipating soil properties due to the varied mineral compositions. They underscored the complexity of using mineral factors for determining origin in Arctic regions, recommending the incorporation of diverse source minerals and alternative techniques such as Fe-Oxide fingerprinting to improve precision.

One of the major challenges is the anthropogenic contamination of soil caused by plants, factories, and the oil industry, which makes predicting soil behavior difficult. For example, from 1954 to 1983, a vermiculite processing plant located near Honolulu airport handled material contaminated with asbestos from the Libby, Montana mine, leading to significant health concerns that eventually caused the facility to shut down in 1983 and undergo remediation in 2001^[10]. Despite these remediation efforts, there remain worries about the persistence of asbestos contamination due to the facility's proximity to residential areas. Recent soil and air sample tests have shown that asbestos contamination remains in the soil, though no airborne asbestos fibers were detected. However, there is still a risk that fibers could become airborne under certain conditions.

Considering that the study area comprises deposits formed by various types of flow, both the type of flow and sediment load significantly influence the mineral content and distribution in the soil. underscores that changes in flow quantity and sediment load components, driven by climatic changes and human activities in river basins, directly impact these characteristics^[11,12]. These dynamics are evident in river delta sediments, facilitating comparisons between the attributes of recent and ancient sediment layers. Furthermore, variations in soil horizons within the same pedon, influenced by pedogenic processes, transportation, and deposition, exhibit distinct properties such as texture, organic matter content, soil pH, redox potential, element content, minerals, oxides, and microbial communities. Therefore, investigating these factors is crucial for understanding the mineral composition and distribution in the studied area^[13,14].

^[15] find The Tigris and Euphrates rivers deposit most of their suspended load in the Mesopotamian Plain, primarily comprising silt, clay, and sand particles. The sediment anal-

ysis revealed that silt particles dominate, with an increase in clay particles further along the rivers. pH values ranged from 7.39 to 7.70, and electrical conductivity from 1.39 to 2.16 ds m⁻¹. The sediments contained 83% non-clay minerals (e.g., calcite, quartz) and 17% clay minerals (e.g., illite, kaolinite). Taking this into account, we have determined that evaluating the soils in the specified area is of great interest and essential due to the high oil industry activities in southern Iraq over the past 70 years, which have undoubtedly affected soil composition. Rahman et al., 2022 The study analyzed heavy mineral (HM) concentrations in Meghna River sands using various microscopic and spectrometric techniques to determine their mineralogy, geochemistry, and source rocks. The sands were primarily composed of quartz and feldspar, with HMs making up around 9 wt.% and including amphibole, epidote, and garnet. Ilmenite and garnet were identified as having commercial extraction potential due to their favorable compositions and concentrations. The sands' textures and feldspar content indicated low hydraulic sorting and alteration, suggesting a mixed metamorphic and igneous source area^[16].

This study aims to assess the soil in terms of silt and oxides at the Shatt al-Arab Deposits in Basra, Iraq, using a mineralogical approach. To the best of our knowledge, there is no study in the literature that evaluates the mineralogy of this specific region for detecting silt and oxides. Samples were collected from depths of 0–30, 30–60, and 60–90 cm. The silt fraction (2–53 micrometers) was isolated, and mineral analysis was conducted using XRD and a point counting device. Morphological characteristics were determined using a polarized light microscope. XRD analysis revealed the presence of minerals such as quartz, calcite, dolomite, smectite, kaolinite, chlorite, illite, hematite, magnetite, and albite at varying depths. Additionally, polarized light microscopy identified further minerals within light and heavy fractions. This comprehensive mineralogical evaluation provides a novel contribution to understanding the soil composition in the Shatt al-Arab region, offering critical insights into the impact of prolonged oil industry activities on soil characteristics.

2. Materials and methods

The study area was chosen within the lands located in Basra Governorate. This area represents part of the southern

alluvial plain of Iraq, where three sites were selected from the study soils **Figure 1**.

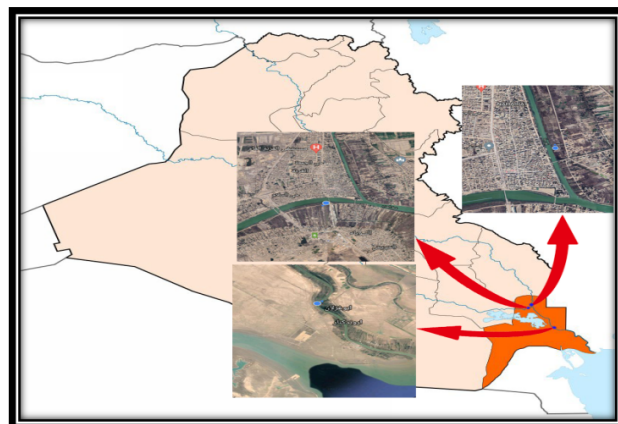


Figure 1. Map of Iraq showing the study areas.

2.1 Preliminary procedures

The study area was selected within the lands located in Basra Governorate, specifically in the Faw area. This area represents part of the southern sedimentary plain of Iraq. Soil samples were obtained uniformly at depths of (0–30 cm, 30–60 cm, and 60–90 cm). The samples were then transported to the laboratory where they were air-dried and disaggregated using a wooden hammer (to preserve the morphology of the minerals). The samples were then sieved with a 2 mm mesh. After that, the silt separates were isolated, and the sand was separated using a 53-micrometer sieve. Finally, clay was separated from silt using the sedimentation method.

2.2 Mineralogical analysis

The X-ray diffraction (XRD) analysis of the silt separates was conducted using the powder method at the Department of Earth Sciences, College of Science, utilizing an X-RD device. The software program used for identifying the predominant sand minerals in the silt separates was (ICDD).

Additionally, minerals were counted and calculated using the point counting method with a polarized light microscope. A slide was prepared with Canada balsam, onto which the silt separates were lightly sprayed, approximately 300 grains per slide. The percentage of each mineral was then calculated and identified. The correlation coefficient between the oxide minerals hematite and magnetite was also calculated.

3. Results and discussion

3.1 X-ray diffraction of Shatt al-Arab deposits in the silt separates

The results of the X-ray diffraction (XRD) analysis, as shown in **Figure 2**, for the Shatt al-Arab deposits at a depth of 0–30 cm in the silt separates, indicated the dominance of Calcite at 38.1%, followed by Quartz at 27.6%, Dolomite at 10.1%, Albite at 6.2%, Smectite at 4.1%, Chlorite at 3.8%, Kaolinite at 3.2%, Magnetite at 3.1%, Hematite at 2.2%, and Illite at 1.5%.

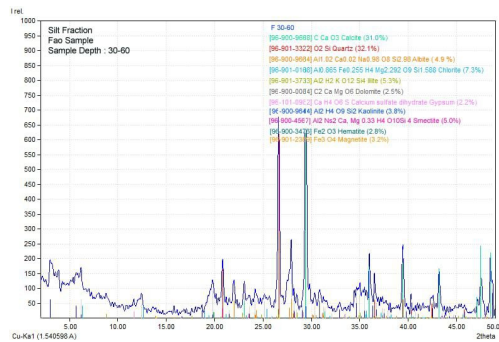


Figure 2. X-ray diffraction of silt for Shatt al-Arab deposits at a depth of 0–30 cm.

The results of the X-ray diffraction (XRD) analysis, as shown in **Figure 3**, for the Shatt al-Arab deposits at a depth of 30–60 cm in the silt separates, indicated the dominance of Quartz at 32.1%, followed by Calcite at 31.0%, Illite at 3.5%, Smectite at 5.0%, Albite at 4.9%, Chlorite at 3.7%, Kaolinite at 8.3%, Magnetite at 3.2%, Hematite at 2.8%, and Dolomite at 2.5%.

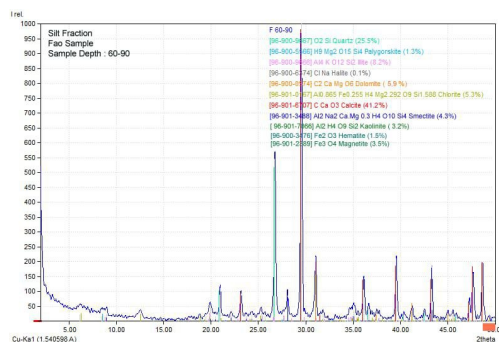


Figure 3. X-ray diffraction of silt for Shatt al-Arab deposits at a depth of 30–60 cm.

The results of the X-ray diffraction (XRD) analysis, as shown in **Figure 4**, for the Shatt al-Arab deposits at a depth

of 60–90 cm in the silt separates, indicated the dominance of Calcite at 41.2%, followed by Quartz at 25.5%, Illite at 8.2%, Dolomite at 5.9%, Smectite at 4.3%, Magnetite at 3.5%, Chlorite at 3.3%, Kaolinite at 3.2%, Hematite at 1.5%, Palygorskite at 1.3%, and Halite at 0.1%.

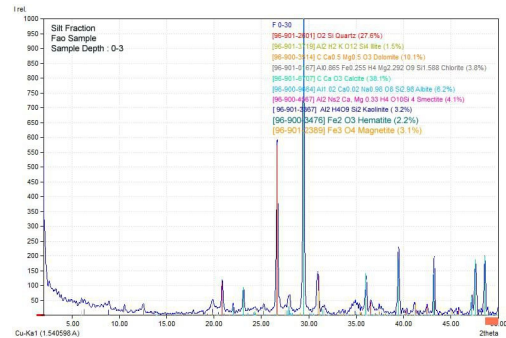


Figure 4. X-ray diffraction of silt for Shatt al-Arab deposits at a depth of 60–90 cm.

From the above results, we find that Quartz dominates at a depth of 30–60 cm, while Calcite dominates at depths of 0–30 cm and 60–90 cm. This is attributed to the calcium-rich parent material, which is the main component of calcareous rocks prevalent in areas with dry and semi-arid climates. Calcite is also found in igneous rocks with low silica content and is absent in regions with high rainfall. The results also showed the presence of Albite at depths of 0–30 cm and 30–60 cm. Albite, a member of the feldspar group, is attributed to the nature of the parent material and the activity of weathering processes^[17].

Dolomite was identified at a depth of 0–30 cm, which is attributed to the mineral composition of the parent material. The results also showed the presence of Chlorite in small amounts at all depths. Illite was found at all depths, a mineral inherited from the parent basaltic rocks, which could be transported to the soil by wind in very small amounts. This mineral can also form under suitable conditions with appropriate potassium concentration in the surface horizon and repeated biological activity. Palygorskite was found at a depth of 60–90 cm, and its formation is attributed to the weathering of parent rocks in dry and semi-arid climatic conditions. Additionally, the results indicated the presence of Magnetite and Hematite at all depths, consistent with the findings of^[18].

Based on the above results, we find a decrease in the percentage with increasing soil depth for the minerals Calcite, Dolomite, Albite, Chlorite, and Hematite. Meanwhile, the

percentage of Quartz, Illite, and Magnetite increased with depth. The percentages of Smectite and Kaolinite varied with increasing soil depth.

3.2 Heavy minerals in the silt separates of Shatt al-Arab deposits

The results in **Table 1** show the percentages of heavy minerals in the silt separates of the Shatt al-Arab deposits. The main minerals identified were primarily from the Opaques group. These minerals were recorded in the silt separates at depths of 0–30 cm, 30–60 cm, and 60–90 cm, with percentages of 31.2%, 30.7%, and 29.3%, respectively.

The Chlorite mineral group was identified with percentages in the silt separates at depths of (0–30, 30–60, and 60–90) cm as 8.4%, 9.9%, and 8.8%, respectively. Chlorite minerals are sheet silicates characterized by their green or brown color and have a glassy or pearly luster. The percentages of heavy minerals less resistant to weathering, represented by Pyroxene, were 6.6%, 5.5%, and 2.5% for the studied depths. Amphiboles, represented by the mineral Hornblende, which is light green and slightly transparent with a slightly greenish-brown hue and a glassy luster^[19], were identified with percentages of 6.5%, 5.6%, and 5.1% for the studied depths.

The examinations also identified the presence of the Mica mineral group within the heavy minerals in the silt separates of the Tigris River deposits. This group includes the minerals Biotite and Muscovite. Biotite was recorded with percentages of 5.4%, 4.9%, and 4.3%, while Muscovite was recorded with percentages of 7.7%, 6.4%, and 9.7%. Generally, Muscovite exceeded Biotite in all depths.

The minerals identified as highly stable included Tourmaline, Zircon, and Rutile, found within the heavy minerals in the silt separates at depths of (0–30, 30–60, and 60–90) cm. The percentages for Tourmaline were 8.8%, 7.3%, and 8.9%, while Zircon recorded 9.2%, 7.5%, and 8.3%. Rutile, characterized by its dark red color and distinct cleavage, had percentages of 6.1%, 7.2%, and 7.4% at the respective studied depths.

Additionally, the heavy minerals in the silt separates included Garnet, which recorded percentages of 2.3%, 4.7%, and 5.5%, while Epidote was identified with percentages of 4.8%, 3.6%, and 5.2% at the respective studied depths.

The results in **Table 1** showed that the heavy minerals

in the silt separates contain Staurolite, which was recorded in the Shatt al-Arab deposits with percentages of 1.5%, 2.4%, and 1.7%. Meanwhile, Kyanite was recorded with percentages of 1.2%, 1.4%, and 2.8% at the respective studied depths.

Figures 5–9 illustrate some images of these minerals.

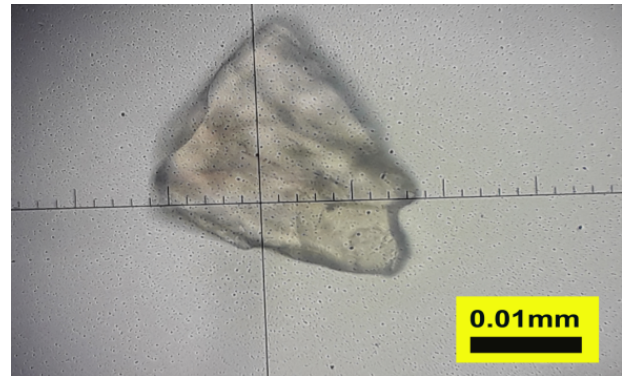


Figure 5. Equidimensional grain with a prominent relief—Garnet in Shatt al-Arab deposits at a depth of 30–60 cm.

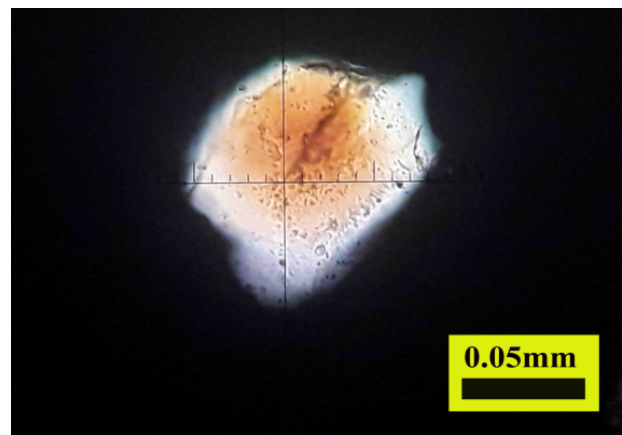


Figure 6. Honey-colored grain—Multicolored strong Tourmaline in Shatt al-Arab deposits at a depth of 30–60 cm.

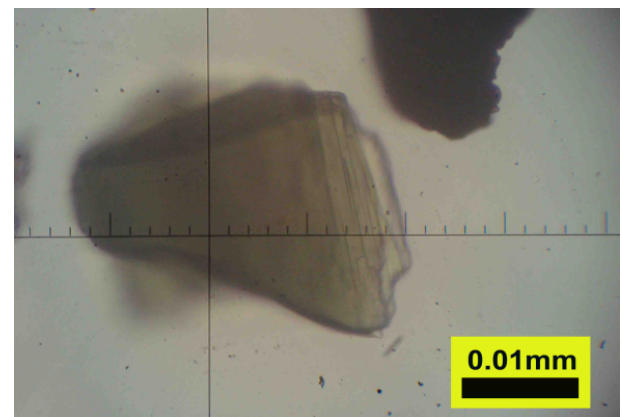


Figure 7. Flaky-shaped grain—Muscovite mica in Shatt al-Arab deposits at a depth of 60–90 cm.

Table 1. Percentages of heavy minerals in the silt separates of Shatt al-Arab deposits.

| Heavy minerals | Shatt al-Arab sediments | | |
|-------------------|-------------------------|-------|-------|
| | 0–30 | 30–60 | 60–90 |
| Opauques | 31.2 | 30.7 | 29.3 |
| Chlorite | 8.4 | 9.9 | 8.8 |
| Pyroxene | 6.6 | 5.5 | 5.2 |
| Hornblende | 6.5 | 5.6 | 5.1 |
| Mica Group | Biotite | 4.9 | 4.3 |
| | Muscovite | 7.7 | 6.4 |
| Epidote | 4.8 | 3.6 | 5.2 |
| Zircon | 9.2 | 7.5 | 8.3 |
| Tourmaline | 8.8 | 7.3 | 8.9 |
| Rutile | 6.1 | 7.2 | 7.4 |
| Garnet | 2.3 | 4.7 | 5.5 |
| Staurolite | 1.5 | 2.4 | 1.7 |
| Kyanite | 1.2 | 1.4 | 2.8 |
| Others | 0.3 | 0.9 | 0.6 |

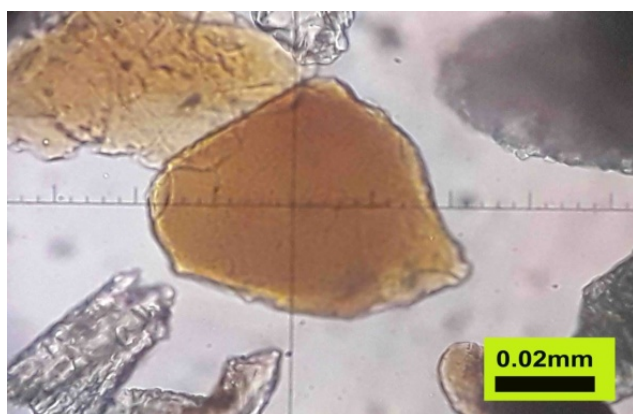


Figure 8. Brown flaky-shaped grain of Biotite mica in Shatt al-Arab deposits at a depth of 60–90 cm.

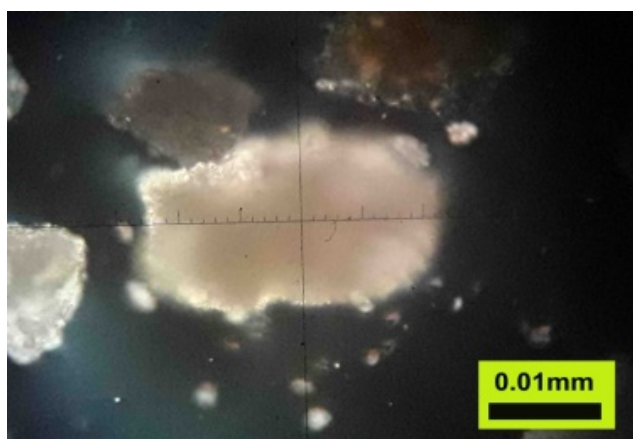


Figure 9. Highly embossed golden grain—Staurolite in Shatt al-Arab deposits at a depth of 60–90 cm.

Light minerals in the silt separates of Shatt al-Arab deposits

The results in **Table 2** show the percentages of light minerals in the silt separates at depths of (0–30, 30–60, and 60–90) cm in the soil of the Shatt al-Arab deposits. The results identified the quartz mineral group, which includes Monocrystalline Quartz and Polycrystalline Quartz. The percentages of Monocrystalline Quartz were 38.2%, 39.3%, and 37.8%, while Polycrystalline Quartz recorded percentages of 4.9%, 3.4%, and 4.2% at the respective studied depths. The dominance of quartz minerals is attributed to their high resistance to weathering, hardness, lack of cracks, and light weight, making them more stable and persistent^[20]. Overall, Monocrystalline Quartz was more dominant compared to Polycrystalline Quartz in all silt separates across the three depths.

The results also showed the dominance of feldspar minerals, represented by Potash Feldspar Microcline and Plagioclase Feldspar, as illustrated in **Figure 10**. These minerals recorded percentages of 3.4% and 4.3% for the above feldspar minerals, respectively, at a depth of 0–30 cm. At depths of 30–60 cm and 60–90 cm, the percentages were 4.1% and 2.8%, and 5.3% and 2.4%, respectively.

The results in **Table 2** showed the rock fragments, which included Carbonate Rock Fragments (**Figure 11**), Chert Rock Fragments, Metamorphic Rock Fragments (**Figure 12**), Evaporites (**Figure 13**), Igneous Rock Fragments,

and Mudstone Rock Fragments. These rock fragments constituted the silt separates at depths of 0–30 cm (16.1%, 8.8%, 6.9%, 8.4%, 2.8%, and 3.1%) respectively. At a depth of 30–60 cm, the percentages were (20.9%, 7.5%, 6.7%, 7.4%, 3.5%, and 2.2%) respectively. At a depth of 60–90 cm, the percentages were (19.2%, 9.4%, 6.7%, 7.3%, 3.2%, and 3.8%) respectively. The dominance of all rock fragments aligns with the findings of Kazem^[9]. The results also showed the dominance of quartz minerals followed by rock fragments, which is consistent with the findings of^[21].



Figure 10. Orthoclase feldspar grain in Shatt al-Arab deposits at a depth of 0–30 cm.

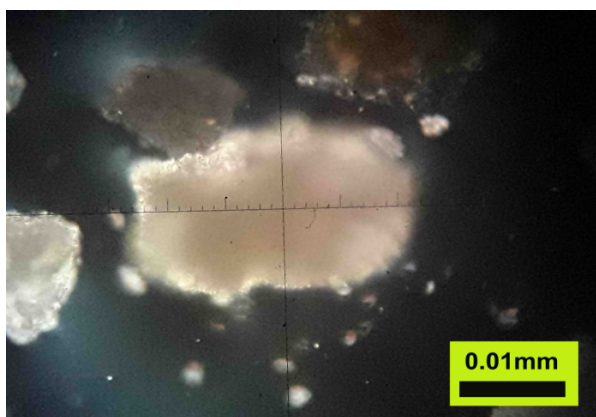


Figure 11. Carbonate rock fragment—limestone in Shatt al-Arab deposits at a depth of 30–60 cm.

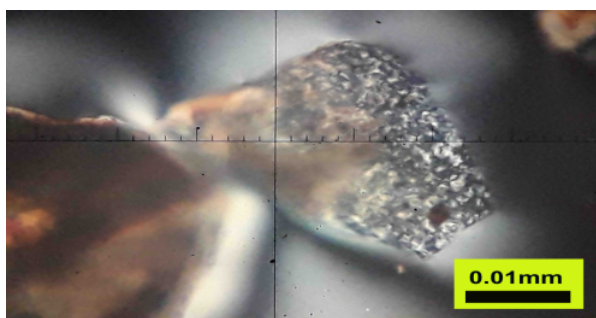


Figure 12. Chert rock fragment in Shatt al-Arab deposits at a depth of 30–60 cm.

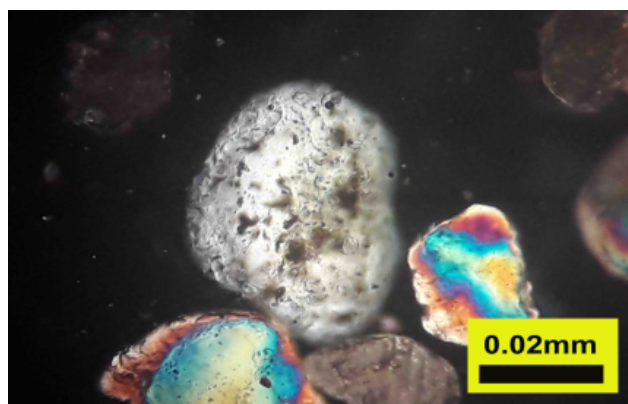


Figure 13. Evaporite rock fragment—gypsum in Shatt al-Arab deposits at a depth of 30–60 cm.

3.3 Free iron oxides in the silt separates of Shatt al-Arab deposits

Table 3 shows the presence of Hematite in the silt separates of Shatt al-Arab deposits at depths of 0–30 cm, 30–60 cm, and 60–90 cm, with percentages of 2.2%, 2.8%, and 1.5%, respectively. This mineral is one of the most important free iron oxides, characterized by its shiny black color and high density, and is part of metamorphic igneous rocks^[22]. The results also showed the presence of Magnetite in the silt separates of Shatt al-Arab deposits at depths of 0–30 cm, 30–60 cm, and 60–90 cm, with percentages of 1.3%, 3.2%, and 5.3%, respectively. The proportions of Magnetite were higher than those of Hematite in these deposits. The total oxides in these separates were 5.3%, 6.0%, and 5.0%, which is consistent with the findings of^[23, 24].

4. Conclusions

This study investigates the mineral composition and distribution of silt and oxides in the Shatt al-Arab River deposits in the Faw area of Basra Governorate. Using XRD and polarized light microscopy, minerals such as quartz, calcite, dolomite, and others were identified at various depths. The findings highlight a dominance of monocrystalline quartz and opaque minerals, with magnetite more prevalent than hematite, and significant depth-related variations. These results provide valuable insights into sedimentary processes and resource potential, emphasizing the need for further research on temporal changes in mineral composition to better understand regional geology and resource management.

Table 2. Percentages of light minerals in the silt separates of Shatt al-Arab deposits.

| Light minerals | Shatt al-Arab sediments | | | |
|------------------------------|----------------------------|-------|-------|------|
| | 0–30 | 30–60 | 60–90 | |
| Quartz | Monocrystalline Quartz | 38.2 | 39.3 | 37.8 |
| | Polycrystalline Quartz | 4.9 | 3.4 | 4.2 |
| Feldspars | Potash Feldspar | 3.4 | 4.1 | 3.5 |
| | Plagioclase Feldspar | 4.3 | 2.8 | 2.4 |
| | Carbonate Rock Fragments | 16.1 | 20.9 | 19.2 |
| Rock | Chert Rock Fragments | 8.8 | 7.5 | 9.4 |
| | Mudstone Rock Fragments | 6.9 | 6.7 | 6.7 |
| | Evaporites (Gypsum) | 8.4 | 7.4 | 7.3 |
| | Igneous Rock Fragment | 2.8 | 3.5 | 3.2 |
| | Metamorphic Rock Fragments | 3.1 | 2.2 | 3.8 |
| Coated Grains by Clay | 2.5 | 1.4 | 2.2 | |
| Others | 0.6 | 0.9 | 0.3 | |

Table 3. Percentage of iron oxides in the silt separates of Shatt al-Arab deposits.

| Mineral % | Depths 0–30 cm | Depths 30–60 cm | Depths 60–90 cm | Correlation |
|-----------|----------------|-----------------|-----------------|-------------|
| Hematite | 2.2 | 2.8 | 1.5 | 0.53 |
| Magnetite | 3.1 | 3.2 | 3.5 | 0.96 |
| Total | 5.3 | 6.0 | 5.0 | |

Author Contributions

All authors contributed equally to all stages of the study, from conceptualization and study design to data collection, analysis, writing of the manuscript, and final approval of the published version.

Conflict of Interest

The Authors declares that there is no conflict of interest.

Data Availability Statement

Data will be available on request from the author.

Funding

This research received no external funding.

Acknowledgments

The author is grateful to College of Agriculture, Al-Qadisiyah University.

References

- [1] Razum, I., Pavlaković, S.M., Rubinić, V., et al., 2024. New soil weathering index based on compositional data analyses of silt to sand sized parent mineral assemblages of terra rossa soils. *Journal of Geochemical Exploration*. 263, 107513. DOI: <https://doi.org/10.1016/J.GEXPLO.2024.107513>.
- [2] Linke, T., Oelkers, E.H., Dideriksen, K., et al., 2024. The geochemical evolution of basalt Enhanced Rock Weathering systems quantified from a natural analogue. *Geochim. Cosmochim. Acta*. 370, 66–77. DOI: <https://doi.org/10.1016/J.GCA.2024.02.005>.
- [3] Jaques, D.S., Marques, E.A.G., Marcellino, L.C., et al., 2021. Morphological and mineralogical characterization of weathering zones in tropical climates: A basis for understanding the weathering process on granitic rocks in southeastern Brazil. *Journal of South American Earth Sciences*. 108, 103187. DOI: <https://doi.org/10.1016/J.JSAMES.2021.103187>.
- [4] Ohta, T., Arai, H., 2007. Statistical empirical index of chemical weathering in igneous rocks: A new tool for evaluating the degree of weathering. *Chemical Geology*. 240, 280–297. DOI: <https://doi.org/10.1016/J.CHEM-GEO.2007.02.017>.
- [5] Durn, G., Rubinić, V., Wacha, L., et al., 2018. Polygenetic soil formation on Late Glacial Loess on

- the Susak Island reflects paleo-environmental changes in the Northern Adriatic area. *Quaternary International*. 494, 236–247. DOI: <https://doi.org/10.1016/J.QUAINT.2017.06.072>.
- [6] Ulery, A., Drees, L.R., 2015. Methods of soil analysis, part 5: Mineralogical methods. *Methods Soil Anal. Part 5 Mineral. Methods*. 5, 1–521. DOI: <https://doi.org/10.2136/sssabookser5.5>.
- [7] Viscarra Rossel, R.A., Bui, E.N., De Caritat, P., et al., 2010. Mapping iron oxides and the color of Australian soil using visible–near-infrared reflectance spectra. *Journal of Geophysical Research: Earth Surface*. 115. DOI: <https://doi.org/10.1029/2009JF001645>.
- [8] Ugochukwu, N., Ali, I.S., Fu, Q., et al., 2012. Sorption of lead on variable-charge soils in China as affected by initial metal concentration, pH and soil properties. *Journal of Food, Agriculture and Environment*. 10(3–4), 1014–1019.
- [9] Myers, W.B., Darby, D.A., 2022. A compilation of the silt and clay mineralogy from coastal and shelf regions of the Arctic Ocean. *Marine Geology*. 454, 106948. DOI: <https://doi.org/10.1016/J.MAR-GEO.2022.106948>.
- [10] Chornkrathok, S., Carbone, M., Yang, H., et al., 2024. Mineralogical investigation of asbestos contamination of soil near old vermiculite processing plant in Honolulu, Hawai‘i. *Environmental Pollution*. 356, 124350. DOI: <https://doi.org/10.1016/J.ENVPOL.2024.124350>.
- [11] Shao, J., Yang, S., Li, C., 2012. Chemical indices (CIA and WIP) as proxies for integrated chemical weathering in China: Inferences from analysis of fluvial sediments. *Sedimentary Geology*. 265–266, 110–120. DOI: <https://doi.org/10.1016/J.SEDGEO.2012.03.020>.
- [12] Li, Y., Zhang, H., Tu, C., et al., 2018. Magnetic characterization of distinct soil layers and its implications for environmental changes in the coastal soils from the Yellow River Delta. *CATENA*. 162, 245–254. DOI: <https://doi.org/10.1016/J.CATENA.2017.11.006>.
- [13] Xiong, S., Ding, Z., Zhu, Y., et al., 2010. A 6 Ma chemical weathering history, the grain size dependence of chemical weathering intensity, and its implications for provenance change of the Chinese loess–red clay deposit. *Quaternary Science Reviews*. 29, 1911–1922. DOI: <https://doi.org/10.1016/J.QUAS-CIREV.2010.04.009>.
- [14] Bockheim, J.G., Hartemink, A.E., 2013. Distribution and classification of soils with clay-enriched horizons in the USA. *Geoderma*. 209–210, 153–160. DOI: <https://doi.org/10.1016/J.GEODERMA.2013.06.009>.
- [15] Al-Shihmani, L. S. S., Al-Shammary, A. A. G., et al., 2024. Physicochemical and mineral properties of suspended sediments of the Tigris and Euphrates rivers in the Mesopotamian Plain. *Science of the Total Environment*. 915, 170066.
- [16] Rahman, M. J. J., Pownceby, M. I., et al., 2022. Distribution and characterization of heavy minerals in Meghna River sand deposits, Bangladesh. *Ore Geology Reviews*. 143, 104773.
- [17] Kazem, M. A., 2017. Classification of Some Soils in the East Shatt Al-Arab Area in Basra Governorate and Evaluation of Land Suitability for Agricultural Purposes Using Remote Sensing Techniques [PhD thesis]. Basrah: University of Basra.
- [18] Sadkhan, M. T., 2014. Sedimentary and mineralogical study of the Hammar Formation in southern Iraq, Um Qasr and Khor Al-Zubair. *Basra Research Journal*. 4(4).
- [19] Barrow, N.J., 1993. Mechanisms of Reaction of Zinc with Soil and Soil Components. *Zinc Soils Plants*. 15–31. DOI: https://doi.org/10.1007/978-94-011-0878-2_2.
- [20] Jha, A.K., Sivapullaiah, P. V., 2017. Unpredictable Behaviour of Gypseous/Gypsiferous Soil: An Overview. *Indian Geotechnical Journal*. 47, 503–520. DOI: <https://doi.org/10.1007/S40098-017-0239-5>.
- [21] Al-Gabban, H. J. and Raid. S. J., 2024. Study of heavy and light minerals and free iron oxides in sand fraction for Tigris and Euphrates rivers/Iraq. Publication in Jundishapur Journal of Microbiology. 15, 5170–5187.
- [22] Viscarra, R. A., Bui, E.N., De Caritat, P., et al., 2010. Mapping iron oxides and the color of Australian soil using visible–near-infrared reflectance spectra. *Journal of Geophysical Research: Earth Surface*. 115, F04031.
- [23] Al-Khafaji, H. A., 2022. Study of the Impact of Carbonate Minerals on the Mineral Composition of the Sediments of the Tigris and Euphrates Rivers [Master’s thesis]. Al Diwaniyah: College of Agriculture, University of Al-Qadisiyah.
- [24] Al-Gabban, H. J., 2022. Study of Mineral Composition and Iron Oxides in the Soils of the Tigris and Euphrates River Sediments [Master’s thesis]. Al Diwaniyah: College of Agriculture, University of Al-Qadisiyah.